trends and links to large-scale patterns. *Nat. Hazards Earth Syst. Sci.* **10**: 1379–1391.

Pant GB, Hingane LS. 1988. Climatic changes in and around the Rajasthan desert during the 20th century. *J. Climatol.* **8**: 391–401.

Park H-S, Chiang JCH, Lintner BR *et al.* 2010. The delayed effect of major El Niño events on Indian monsoon rainfall. *J. Clim.* **23**: 932–946.

Pettitt A. 1979. A non-parametric approach to the change-point problem. *Appl. Stat*. **28**(2): 126–135.

Rana A, Uvo CB, Bengtsson L *et al.* 2011. Trend analysis for rainfall in Delhi and Mumbai, India. *Clim. Dyn.* **38**: 45–56.

Rao AR, Hamed KH, Chen H-L. 2003. *Nonstationarities in Hydrologic and Environmental Time Series*, Kluwer Academic: Dordrecht, the Netherlands.

Roy S. 2006. The impacts of Enso, PDO, and local SSTs on winter precipitation in India. *Phys. Geogr.* **27**: 464–474.

Schepen A, Wang QJ, Robertson D. 2012. Evidence for using lagged climate indices to forecast Australian seasonal rainfall. *J. Clim.* **25**: 1230–1246.

Shukla J, Paolino DA. 1983. The Southern oscillation and long-range forecasting of the summer monsoon rainfall over India. *Mon. Weather Rev.* **111**: 1830–1837.

Simon A, Mohankumar K. 2004. Spatial variability and rainfall characteristics of Kerala. *J. Earth Syst. Sci.* **113**: 211–221.

Singh PO, Khan MTA, Rahman S. 2001. Has the frequency of intense cyclones increased in the north Indian ocean? *Curr. Sci.* **80**: 575–580.

Sivaperuman C, Baqri QH, Ramaswamy G *et al.* (eds) 2009. *Faunal Ecology and Conservation of the Great Indian Desert*. Springer: Berlin and Heidelberg, Germany

Slingo JM, Annamalai H. 2000. The El Niño of the century and the response of the Indian summer monsoon. *Mon. Weather Rev.* **128**: 1778–1797.

Stone RC, Hammer GL, Marcussen T. 1996. Prediction of global rainfall probabilities using phases of the Southern Oscillation Index. *Nature* **384**: 252–255.

Torrence C, Webster P. 1999. Interdecadal changes in the ENSO–Monsoon System. *J. Clim.* **12**: 2679–2690.

Tripathi CK, Rai S, Pandey CA *et al.* 2008. Southern Indian Ocean SST indices as early predictors of Indian Summer monsoon. *Indian J. Mar. Sci.* **37**: 70–76.

Wang X, Wang C, Zhou W *et al.* 2010. Teleconnected influence of North Atlantic sea surface temperature on the El Niño onset. *Clim. Dyn.* **37**: 663–676.

Xie S-P, Du Y, Huang G *et al.* 2010. Decadal shift in El Niño influences on Indo–Western Pacific and East Asian climate in the 1970s. *J. Clim.* **23**: 3352–3368.

Yadav RK, Yoo JH, Kucharski F *et al.* 2010. Why is ENSO influencing northwest India winter precipitation in recent decades? *J. Clim.* **23**: 1979–1993.

Yue S, Pilon P, Phinney B *et al.* 2002. The influence of autocorrelation on the ability to detect trend in hydrological series. *Hydrol. Process.* **16**: 1807–1829.

Supporting information

Figure S1. Biplots from PCA for (Aj) during MAM, and (Am) during MAM, in pre- and post-shift years.

Correspondence to: Kamna Sachdeva

kamna.sachdeva@teri.res.in

doi:10.1002/wea.2746

Contrail lobes or mamma? The importance of correct terminology

David M. Schultz[1] and Y. Hancock[2]

[1]School of Earth, Atmospheric and Environmental Sciences, Centre for Atmospheric Science, University of Manchester

[2]Department of Physics and the York Centre for Complex Systems Analysis, University of York

Contrails are clouds formed by aircraft (Glossary of Meteorology, 2000). A contraction of the two words *condensation trails*, contrails are the result of water vapour formed from combustion in the aircraft engines during flight, which is then exhausted, cooled, and condensed. They were first observed in the early days of aviation (see http://contrailscience.com/pre-wwii-contrails/), with some of the initial scientific reports documented in *Scientific American* (Well, 1919), *Monthly Weather Review* (Varney, 1921a; 1921b), and *Nature* (1930) – the last referring to them as a 'Historic Natural Event'. (These and other early reports are collated and discussed in Baucom (2007a).) Alfred Wegener, originator of the theory of continental drift, used his observations of the 22° halo from contrails to argue that they were clouds made of ice crystals, not smoke from exhaust (Wegener, 1921). Later during World War II, contrails became a feared sign of impending air-attacks and resulted in extensive military research to understand them (Baucom, 2007b).

With over 100 000 commercial flights each day (Air Transport Action Group, 2014), the potential for a large anthropogenic impact on cloud formation in the upper troposphere is possible, altering the radiative balance of the Earth. One estimate is that an annual-averaged 0.13% of the Northern Hemisphere is covered in contrails (Duda *et al.*, 2013), and another is that 6% of Arctic surface warming to date has been caused by contrails (Jacobson *et al.*, 2013).

Not all aircraft will produce contrails, as their formation depends upon several factors: the number of aircraft engines (Sussmann and Gierens, 2001), amount of exhausted vapour, environmental relative humidity and temperature, air pressure, and the aircraft's propulsion efficiency. Once formed, contrails can undergo a variety of different evolutions (e.g. Scorer, 1972; Mazón *et al.*, 2012). Some contrails evaporate immediately. Other contrails do not evaporate within 10 minutes (so-called persistent contrails); rather, they will often expand and grow in mass to develop into cirrus clouds (e.g. Schröder *et al.*, 2000; Atlas *et al.*, 2006; Heymsfield *et al.*, 2010). Persistent contrails are found to limit, for example, ground-based astronomy (Livingston, 1969). Although some contrails maintain a linear structure until they evaporate, others evolve to develop characteristic regions of lobular cloud (Figure 1). This article pertains to these characteristic lobes, their dynamics, and their classification.

Contrail is the official cloud name, appearing in the World Meteorological Organization's Cloud Atlas (1975; 1987). *Cirrus aviaticus,* as is sometimes seen online in nonscientific contexts, has an unknown origin and is not official. The lobular cloud regions in contrails have been variously called 'drop-like formations' and 'pendulous lumps' (Ludlam and Scorer, 1953), 'blobs' (Scorer and Davenport, 1970), 'pendant swellings like inverted mushrooms' (World Meteorological Organization, 1975, p. 66), 'pendules or fingers' (Schaefer and Day, 1981, p. 138), 'puffs' (Lewellen and Lewellen, 2001), 'clumps of condensate' (Rossow and Brown, 2010), 'smoke rings' (Unterstrasser *et al.,* 2014), and 'tear-drop structures' (Paoli and Shariff, 2016). They have also been called 'mammatus' (Ludlam and Scorer, 1953; Schultz *et al.,* 2006; Unterstrasser *et al.,* 2014), 'akin to mammato-cumulus' (Day and Schaefer, 1998), and 'mamma structures' (Paoli and Shariff, 2016). This discrepancy in terminology in the literature (as well as public-facing websites discussing contrails and meteorology) raises an important question as to what should be the appropriate scientific name for these features. This question is more than one of minor academic interest.

Cloud types have been codified in the *International Cloud Atlas* in part to ensure uniformity in terminology despite the different languages and cultures of observers worldwide (World Meteorological Organization, 1975; 1987). Cloud names also imply a meaning about their formation, maintenance, composition, and dynamics that goes beyond the specific term describing the cloud's appearance. For example, the term *cumulus humilis* not only paints a picture of a fair-weather puffy cloud, but it is also associated with the definition that, within this convective cloud, individual parcels exist that are only buoyant for a shallow depth before reaching their equilibrium level. Similarly, establishing correct terminology for the distinct, lobular regions of contrails needs to benefit those classifying clouds and cloud formations, and also to serve the purpose of remaining faithful to and descriptive of the physics that creates them. In this respect, we deem general terminology for the lobular cloud regions in contrails (e.g. puffs, blobs) to be insufficient. In this article, we also examine the use of the specific term *mamma* for these features, and ask whether the physical processes responsible for contrail lobe formation resemble those of mamma. If so, then calling them contrail mamma is justified; otherwise, a separate terminology to distinguish their unique formation processes should be created. (We use the term *mamma* in this article, which is the accepted terminology from the *International Cloud Atlas,* rather than the more popular and common term *mammatus.*)

To provide context to this issue, we present a key example of characteristic lobes in several persistent contrails that occurred over northern England. We discuss the origin of the terminology associated with these features, their dynamics, and possible research questions for the scientific community.

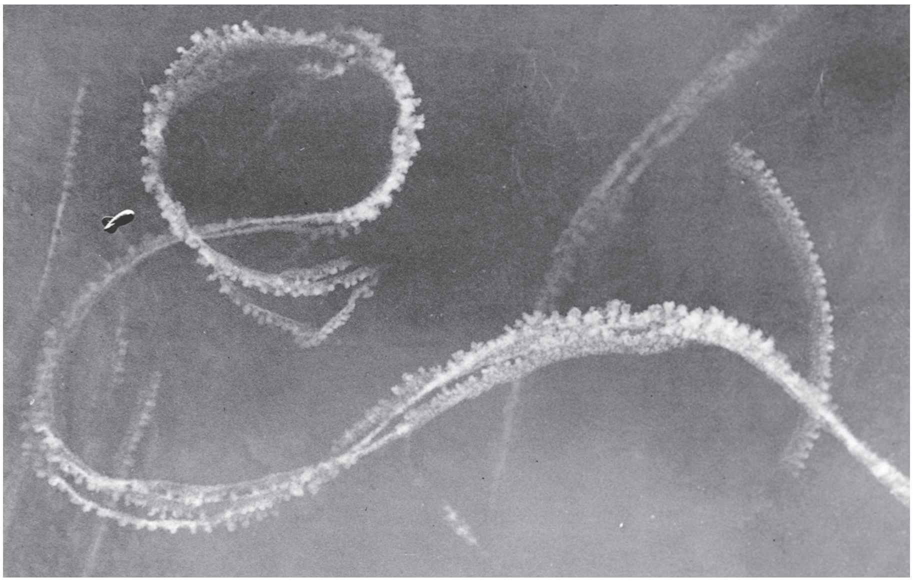

Figure 1. Dramatic condensation trails from German and British fighter planes engaged in aerial combat over Kent on 3 September 1940. (Copyright Press Association.)

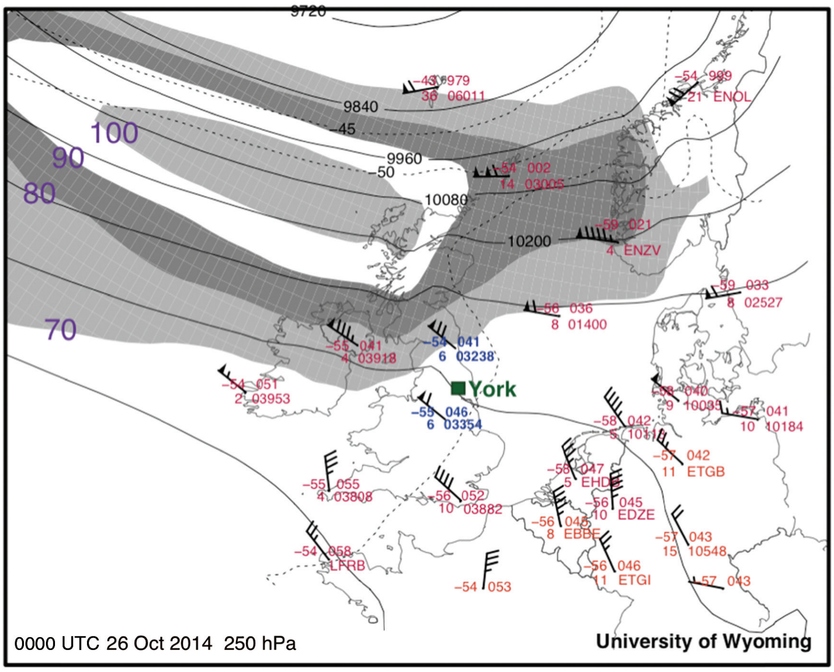

Figure 2. The 250hPa constant pressure chart over the UK and northwestern Europe at 0000 UTC *on 26 October 2014. The station model contains air temperature (°C, upper left), abbreviated geopotential height (m, leading '9' or '10' omitted, upper right), dewpoint depression (degC, lower left), and WMO station number or ICAO location indicator (lower right). Blue station models are for Albermarle (03238) and Nottingham (03354). A green square represents the location of York where the photographs were taken. One pennant, full barb and half-barb denote 50, 10, and 5kn, respectively. Analysis of 250hPa wind speed (kn, shaded), geopotential height (solid lines every 120m), and air temperature (dashed lines every −5°C) from the Global Forecast System (GFS) model. (Redrafted from data and plots provided by the University of Wyoming http://www.weather.uwyo.edu/upperair/uamap.html.)*

Contrails on 25 October 2014

In the late afternoon, a remarkable display of contrails was observed west of York, UK. Photographs of the contrails were taken along the River Ouse, looking to the southwest and west. The surface conditions at the University of York observing station (see http://weather.elec.york.ac.uk/live-graphs.html) were a temperature of 13°C, dewpoint temperature of 8°C (relative humidity of 70%), southwest winds of about 13kn, and increasing surface pressure. The synoptic situation featured a low-pressure centre moving eastward to the north of the UK, placing the UK in the right-exit region of the jet stream (Figure 2). Cloud cover was increasing from the west as a cold front approached the UK from the north. Such observations are consistent with previous reports that have shown jet-exit regions and approaching cold fronts to be favourable synoptic conditions for persistent contrails (Carleton *et al.,* 2008; Laken *et al.,* 2012).

At around 16:30 LT (1530 UTC), several aircraft contrails were formed from passenger jets flying primarily northward or southward (Figure 3). Flightradar24.com showed that jets flying around this time were between 9.1km (30 000ft) and 11.5km (39 000ft). The contrails that were produced were initially relatively narrow and continuous (topmost contrail in Figure 3). Within a few minutes, the contrails broadened, forming a brighter band on the underside (e.g. second topmost contrail in Figure 3). Descending lobes developed from within these brighter bands (third topmost contrail in Figure 3), first forming quasi regularly spaced clumps of brighter cloud that then separated from the base of the contrail (Figure 4(a)). After a few minutes, the clumps developed the characteristic shape of these well-developed lobes (Figure 4(b) and (c)). Some of the lobes descended quite far from the contrail, a distance almost half as far as the contrail was deep (Figure 4(c)). None of the observed lobes were observed to separate from the contrails.

The contrails lasted for tens of minutes before evaporating or being covered up by a lower cloud layer (estimated at about 1.5–2km in altitude, Figure 5), allowing for dramatic photographs of lobe-laden contrails extending across a large expanse of the sky. One of the contrails, which was quite different compared with the others, formed Kelvin–Helmholtz waves on top and what looked like highly sheared fallstreaks underneath (Figure 6).

Soundings are needed to understand the atmospheric environment in which these contrails formed. Unfortunately, the closest soundings in space and time were the 0000 UTC 26 October soundings from Albermarle 03238 and Nottingham 03354 (Figures 2 and 5), as there were no 1200 UTC soundings on that day. The 0000 UTC soundings were remarkably similar in wind, temperature, and moisture structure to a model-derived sounding from the real-time ManUniCast forecast model (Schultz *et al.*, 2015) for 1500 UTC, available from http://www.manunicast.com.

Between 9.8 and 11.5km (275–210hPa; 32 000–37 000ft), the air at both Albermarle and Nottingham was about 48% relative humidity with a potential temperature of 325–328K, and winds were about 75kn (39ms^{-1}) from 295 to 300° (Figure 5). Between 9.1 and 9.8km, however, the air at these two stations was quite different. Albermarle to the north had a dry layer (12% relative humidity, air temperature of −53°C and potential temperature of 320–323K) that extended down to about 8.1km (350hPa) with a wind speed veering with height from 60kn (31ms^{-1}) at 281° (9km) to

Figure 3. Photograph taken at York, looking south-southwest, at 1529 UTC on 25 October 2014 of four persistent contrails. The topmost contrail is being created by an aircraft moving from right to left. The second and third topmost contrails are developing contrail lobes.

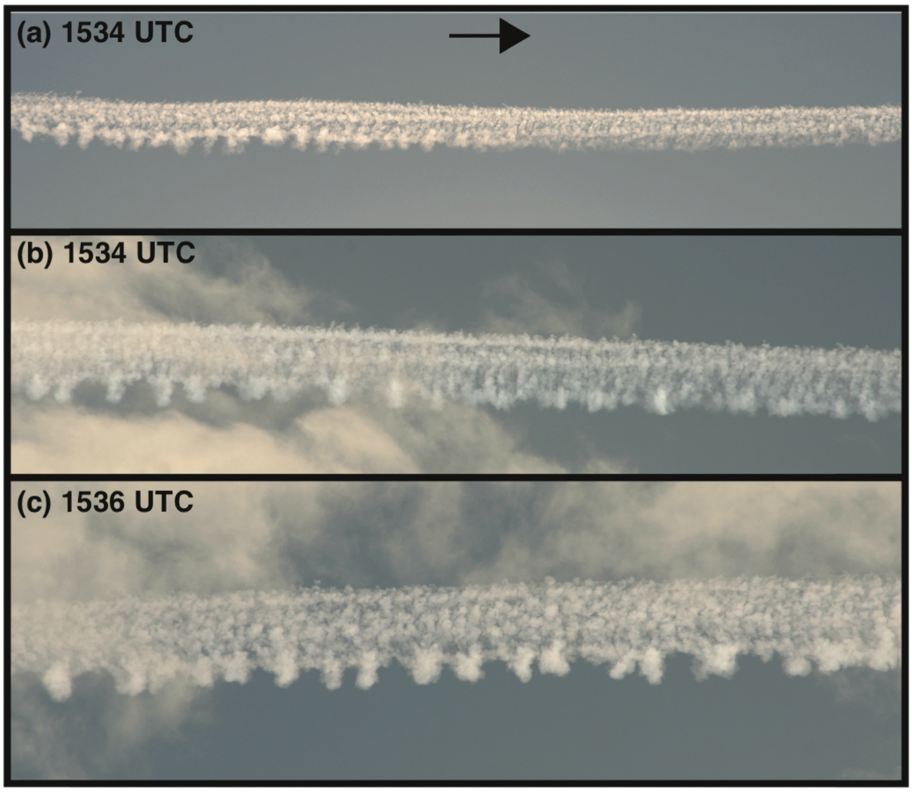

Figure 4. Evolution of a single persistent contrail to produce lobe features along different sections of the contrail, looking south-southwest at York on 25 October 2014: (a) 1534 UTC, (b) 1534 UTC, and (c) 1536 UTC. The arrow indicates the direction of motion of the aircraft that created the contrail.

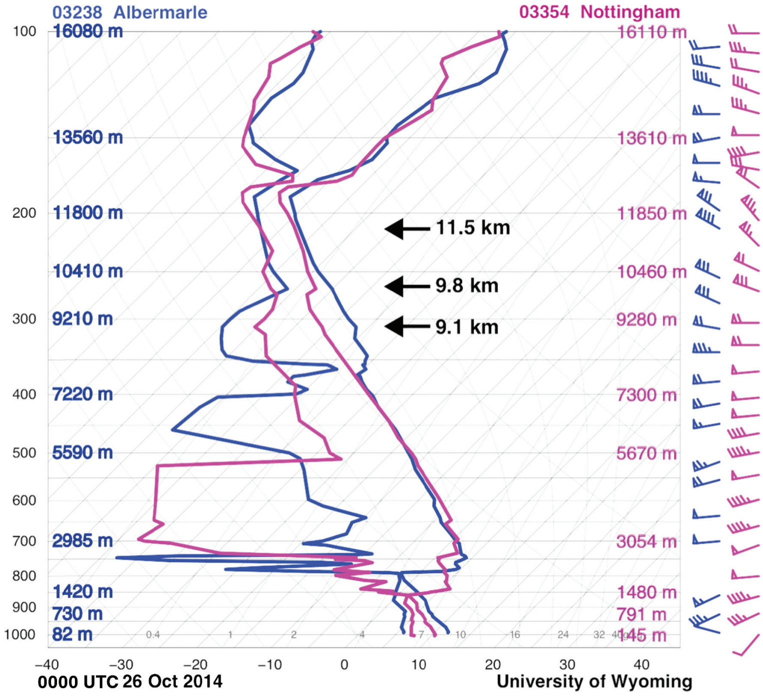

Figure 5. Soundings of temperature, dewpoint temperature, and wind from 0000 UTC on 26 October 2014 at Albermarle (blue) and Nottingham (purple). One pennant, full barb and half-barb denote 50, 25, and 5kn, respectively. Heights discussed in the text are labeled with black arrows. (Redrafted from data and plots provided by the University of Wyoming http://www.weather.uwyo.edu/upperair/sounding.html.)

Figure 6. Photo taken in York of Kelvin–Helmholtz waves on the top of a contrail and possible fallstreaks on the bottom, at 1536 UTC on 25 October 2014, looking west-southwest.

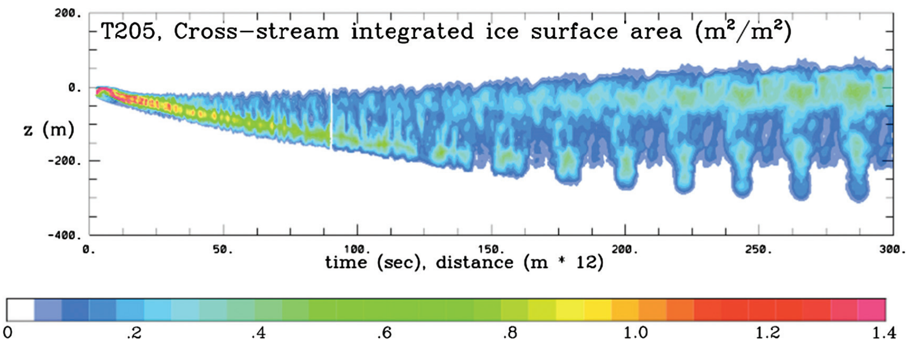

Figure 7. Drift plot of the integrated ice surface area from a 3.6km long segment of a contrail created by a three-dimensional large-eddy numerical model (Fig. 5 in Lewellen, 2014).

75kn at 295° (9.8km). This layer at the more southerly station of Nottingham (a distance of 234km away) was instead characterised by a relative humidity of about 40%, air temperature of −45 to −50°C, potential temperature of 317–320K, and wind direction of 270° at about 60kn (31ms^{-1}). The warmer, drier layer at Albermarle is likely associated with descent in the upper troposphere, occurring in the right-exit region of the jet stream (Figure 2), which is at the altitude where the contrails formed (9.1–11.5km).

At such temperatures (around −50°C), all hydrometeors in the cloud were likely ice particles, consistent with the fuzzy appearance of the contrails a few minutes after being formed (Figure 3). Not much more can be said about the size, concentrations, and habits of the ice particles because of the lack of in situ observations of the contrails.

How do contrail lobes form?

Scorer (1955; 1972) and Scorer and Davenport (1970) provide an explanation for the formation of the contrail lobes from the interaction between two counter-rotating vortices cast by the aircraft. They hypothesised that, where these vortices interact, they produce descending lobes due to mutual amplification. This explanation was shown to be incorrect by Lewellen and Lewellen (1996), who later modelled the evolution of the contrail lobes using a three-dimensional large-eddy simulation model with a passive tracer representing the cloudy exhaust. Their simulations showed that the two counter-rotating vortex tubes formed by the aircraft jet are subject to an instability identified by Crow (1970), in a manner similar to that proposed by Scorer and Davenport (1970). This instability causes the two vortices to bend towards each other at quasi regularly spaced intervals, tens to a few hundred metres apart. Eventually, these bending vortices merge at these points, creating a series of ring vortices. Once formed, the vorticity in these rings advects the rings downward relative to the flight level (similar to smoke rings). Eventually, the descent rate slows as the rings weaken, terminating tens to a few hundred metres below the aircraft flight level. The descended cloud remains visible as the condensate is trapped within the vortical circulations.

Later experiments with increasing sophistication of ice microphysics confirmed these initial simulations (Lewellen and Lewellen, 2001; Lewellen, 2014; Lewellen *et al.*, 2014), and showed that the dynamics of the interacting vortices was the dominant effect that produces the contrail lobes, with ice microphysics being of secondary importance. As an example, Figure 7 shows a drift plot that captures the space and time structure of a 3.6km long segment of contrail created by a three-dimensional large-eddy numerical model (Lewellen, 2014). The quantity plotted – integrated ice surface area – is a measure of the brightness of the contrail cloud and represents an easy way to visualise the cloud that surrounds the vorticity structures. The lobes form underneath the

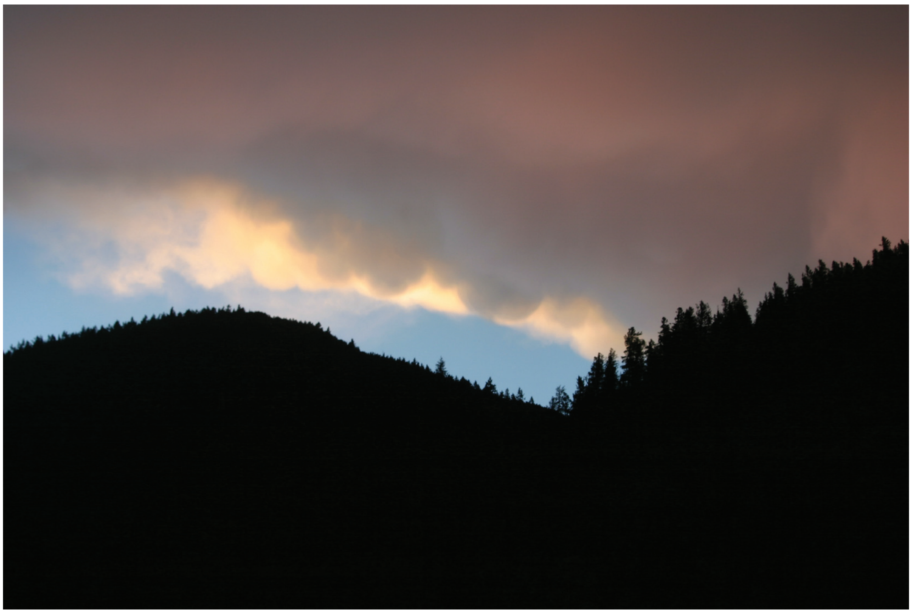

Figure 8. Mamma formations on the underside of a cumulonimbus in Taos, New Mexico, USA on 14 August 2004.

contrail after about 200s (2.4km behind the plane). Other researchers have also simulated contrail lobes, confirming the essence of these results (e.g. Paugam *et al.*, 2010; Naiman *et al.*, 2011; Unterstrasser, 2014; Unterstrasser *et al.*, 2014; Picot *et al.*, 2015). With this large body of literature that has simulated and explained contrail lobe formation, we find it confusing that Paoli and Shariff (2016, p. 419) have subsequently asked, *What is the mechanism of the intriguing and often-observed mamma structures…? Are they … the result of vortex loops formed after vortex reconnection?* Indeed, they are. Thus, the contrail lobes are a result of the vorticity generated by the aircraft and the subsequent evolution of that vorticity.

Because the contrail lobes are formed from the interaction of the counter-rotating vortices behind the plane, those that fly horizontally in the absence of wind shear will produce descending lobes, relative the ground. If the plane were turning, the vortex system and the resulting lobes will be directed outward along the radius of curvature. This process is captured in the photograph in Figure 1, which likely has been taken looking upward at contrails formed from aerial dogfights during World War II. Another way that contrail lobes produced by a level-flying aircraft would not appear to be descending towards the ground is if there is wind shear below the contrail.

How do mamma form?

If that is how lobular structures form on contrails, then how do mamma form? Mamma are bulbous protuberances on cloud bases that make for dramatic photographs when the undersides of the clouds are illuminated by the setting sun (Figure 8). Ley (1894, pp. 84–86, 104) is believed to have first named them. Classified as supplementary features rather than a separate cloud type (World Meteorological Organization, 1987, p. 27; Met Office, 2000, p. 28), mamma are most commonly associated with the underside of anvils of cumulonimbus, although mamma are known to occur on the underside of stratocumulus, altostratus, altocumulus, and cirrus. Individual mamma lobes have smooth mushroom-shaped circulations with a central downdraft and returning upward circulation around the edges (Winstead *et al.*, 2001; Kanak *et al.*, 2008). Historically, the ominous appearance of mamma in cumulonimbus clouds led to the belief that mamma were associated with severe weather (e.g. Humphreys, 1912), although that association has now been discredited (e.g. Schultz *et al.*, 2006).

Many explanations have been proposed for the formation of mamma, but few have been verified as actually producing these structures. Schultz *et al.* (2006) reviewed the scientific literature and identified ten separate mechanisms, including the subsidence of anvils, subcloud evaporation/sublimation, melting, fallout of hydrometeors, cloud-base detrainment instability, radiative effects, gravity waves, Kelvin–Helmholtz instability, Rayleigh–Taylor instability, and Rayleigh–Bénard-like convection. Doswell (2008) proposed an eleventh possible mechanism (double-diffusive convection), but the evidence was evaluated by Schultz *et al.* (2008) and the mechanism was not shown to be valid.

Of these ten mechanisms, Schultz *et al.* (2006) found that most of them could not explain the observed features of mamma and were inconsistent with the environment in which mamma have been observed to form. Only two mechanisms have been tested using models and observations. The first mechanism is cloud-base detrainment instability that relies on subcloud evaporation/sublimation as proposed by Emanuel (1981). Using cloud-model simulations that abstract the soundings from four observed mamma cases, Kanak *et al.* (2008) showed that cloud-base detrainment instability was a necessary, but not sufficient, criterion for the formation of mamma. This instability was favoured by larger lapse rates (or greater static instability) below the cloud base. Kanak *et al.* (2008) also found that drier air beneath the cloud was better for producing well-developed mamma. The second mechanism that has been tested was associated with the radiative temperature contrasts between the cloud base and a dry lower troposphere that destabilises cloudy air and produces a well-mixed layer (Garrett *et al.*, 2010). The mamma are then visible as the descending branches of the positively buoyant lobes of dry air into the cloud. In the real atmosphere, mamma may be formed by one or both of these two mechanisms. In both of these cases, the instability is driven by the growth of small perturbations resulting from unstable thermodynamic differences across or beneath the cloud.

Conclusion

The discussion above reveals the critical difference between contrail lobes and mamma. Whereas contrail lobes are fundamentally defined by dynamic instabilities of the vorticity, mamma structures evolve primarily from thermodynamic instabilities driven by evaporation, radiation, or both. Although at first contrail structures may vaguely resemble mamma, upon closer inspection they are different. Contrail lobes and mamma have a kinematic similarity: they both contain descending vortex rings from a larger cloud (although banked aircraft can produce vortex rings with other orientations relative to the ground observer; Figure 1). This kinematic similarity, however, does not mean that they should be considered similar features, just as dust devils and tornadoes should not be considered the same phenomenon, despite having similar kinematic flow structures. Thus, we advocate that lobes in contrails are not referred to as mamma, and that the contrail and cloud communities should decide upon a common term for consistent use and improved clarity in the communication and definition of these features. In this respect, contrail lobes would be distinguished from mamma, as both have different origins, structures, and evolutions.

In this article, we have used the term *contrail lobe* or *lobular structure* with the term *lobe* being derived from its anatomical definition, specifically, *a major division*

RMetS Royal Meteorological Society

of an organ or part of an organ, especially one having a rounded form and often separated from other lobes by fissures or bands of connective tissue. For example, the brain, liver, and lung are divided into lobes (*Oxford Concise Medical Dictionary*, 2015). We propose that this term is appropriate for these contrail structures and may be considered for possible adoption.

Beyond the issue with the lack of a consistent terminology, future research could involve the study of contrail evolutions to better understand the interactions between the dynamics the thermodynamics of the environment, and the secondary role of cloud microphysics in producing the broad palette of contrail morphologies and evolutions. In this respect, we support the call by Paoli and Shariff (2016, p. 420) for the involvement of citizen-science projects. Although past work has mainly focused on citizen-science observers recording contrail occurrence (Chambers and Duda, 2005; Fowler *et al.*, 2013), the existence of the contrail lobes themselves was not classified by the observers. Although phase spaces exist for the formation of contrails (e.g. Scorer and Davenport, 1970; Paoli and Shariff, 2016), a phase space for the evolution of contrail structures has not yet been developed. Obtaining these data and linking them to the environmental conditions would be a useful exercise for creating a phase space of contrail evolution, which could later validate idealised numerical simulations.

Acknowledgements

Partial funding for Schultz comes from the UK Natural Environment Research Council to NE/1024984/1 at the University of Manchester. We thank the University of Wyoming, in particular Larry Oolman, for the upper-air plots and data. We thank David Lewellen, Mick West, and Vladimir Janković for their discussions and for providing resources about contrails. David Lewellen and an anonymous reviewer provided comments that improved an earlier version of this manuscript.

References

Air Transport Action Group. 2014. Aviation benefits beyond borders. http://aviationbenefits.org/media/26786/ATAG__AviationBenefits2014_FULL_LowRes.pdf (accessed 16 February 2016).

Atlas D, Wang Z, Duda DP. 2006. Contrails to cirrus—Morphology, microphysics, and radiative properties. *J. Appl. Meteorol. Climatol.* **45**: 5–19.

Baucom DR. 2007a. Wakes of war: contrails and the rise of air power, 1918–1945 Part I–early sightings and preliminary explanations, 1918–1938. *Air Power Hist.* **54**(2): 16–31.

Baucom DR. 2007b. Wakes of war: contrails and the rise of air power, 1918–1945 Part II–the air war over Europe, 1939–1945. *Air Power History* **54**(3): 5–21.

Carleton AM, Travis DJ, Master K *et al.* 2008. Composite atmospheric environments of jet contrail outbreaks for the United States. *J. Appl. Meteorol. Climatol.* **47**: 641–667.

Chambers LH, Duda DP. 2005. Count-a-thon of airplane contrails. *Eos Trans. AGU* **86**: 382–383.

Crow SC. 1970. Stability theory for a pair of rotating vortices. *AIAA J.* **8**: 2172–2179.

Day JA, Schaefer VJ. 1998. *Peterson First Guide to Clouds and Weather*, 2nd Edition. Houghton Mifflin Harcourt: New York, NY.

Doswell CA III. 2008. Comments on "The mysteries of mammatus clouds: observations and formation mechanisms". *J. Atmos. Sci.* **65**: 1093–1094.

Duda DP, Minnis P, Khlopenkov K *et al.* 2013. Estimation of 2006 Northern Hemisphere contrail coverage using MODIS data. *Geophys. Res. Lett.* **40**: 612–617.

Emanuel KA. 1981. A similarity theory for unsaturated downdrafts within clouds. *J. Atmos. Sci.* **38**: 1541–1557.

Fowler A, Whyatt JD, Davies G *et al.* 2013. How reliable are citizen-derived scientific data? Assessing the quality of contrail observations made by the general public. *Trans. GIS* **17**: 488–506.

Garrett TJ, Schmidt CT, Kihlgren S *et al.* 2010. Mammatus clouds as a response to cloud-base radiative heating. *J. Atmos. Sci.* **67**: 3891–3903.

Glossary of Meteorology. 2000. Condensation trail. American Meteorological Society. http://glossary.ametsoc.org/wiki/Condensation_trail (accessed 8 March 2016).

Heymsfield A, Baumgardner D, DeMott P *et al.* 2010. Contrail microphysics. *Bull. Am. Meteorol. Soc.* **91**: 465–472.

Humphreys WJ. 1912. Mammato-cumulus clouds. *Mon. Weather Rev.* **40**: 967–968.

Jacobson MZ, Wilkerson JT, Naiman AD *et al.* 2013. The effects of aircraft on climate and pollution. Part II: 20-year impacts of exhaust from all commercial aircraft worldwide treated individually at the subgrid scale. *Faraday Discuss.* **165**: 369–382.

Kanak KM, Straka JM, Schultz DM. 2008. Numerical simulation of mammatus. *J. Atmos. Sci.* **65**: 1606–1621.

Laken BA, Pallé E, Kniveton DR *et al.* 2012. Contrails developed under frontal influences of the North Atlantic. *J. Geophys. Res.* **117**: D11201.

Lewellen DC. 2014. Persistent contrails and contrail cirrus. Part II: full lifetime behavior. *J. Atmos. Sci.* **71**: 4420–4438.

Lewellen DC, Lewellen WS. 1996. Large-eddy simulations of the vortex-pair breakup in aircraft wakes. *AIAA J.* **34**: 2337–2345.

Lewellen DC, Lewellen WS. 2001. The effects of aircraft wave dynamics on contrail development. *J. Atmos. Sci.* **58**: 390–406.

Lewellen DC, Meza O, Huebsch WW. 2014**.** Persistent contrails and contrail cirrus. Part I: large-eddy simulations from inception to demise. *J. Atmos. Sci.* **71**: 4399–4419.

Ley WC. 1894. *Cloudland*. Edward Stanford: London.

Livingston WC. 1969. Aircraft and cloud formation. *Weather* **24**: 56–60.

Ludlam FH, Scorer RS. 1953. Reviews of modern meteorology—10: convection in the atmosphere. *Q. J. R. Meteorol. Soc.* **79**: 317–341.

Mazón J, Costa M, Pino D *et al.* 2012. Clouds caused by human activities. *Weather* **67**: 302–306.

Met Office. 2000. *Observer's Handbook*, 4th Edition, Report 1028. Met Office: Bracknell, UK.

Naiman AD, Lele SK, Jacobson MZ. 2011. Large eddy simulations of contrail development: sensitivity to initial and ambient conditions over first twenty minutes. *J. Geophys. Res.* **116**: D21208.

Nature. 1930. Historic natural events. *Nature* **125**: 692–693.

Martin EA. (ed.) 2015. *Oxford Concise Medical Dictionary*, 9th Edition. Oxford University Press: Oxford, UK.

Paoli R, Shariff K. 2016. Contrail modeling and simulation. *Annu. Rev. Fluid Mech.* **49**: 393–427.

Paugam R, Paoli R, Cariolle D. 2010. Influence of vortex dynamics and atmospheric turbulence on the early evolution of a contrail. *Atmos. Chem. Phys.* **10**: 3933–3952.

Picot J, Paoli R, Thouron O *et al.* 2015. Large-eddy simulation of contrail evolution in the vortex phase and its interaction with atmospheric turbulence. *Atmos. Chem. Phys.* **15**: 7369–7389.

Rossow VJ, Brown AP. 2010. Effect of jet-exhaust streams on structure of vortex wakes. *J. Aircr.* **47**: 1076–1082.

Schaefer VJ, Day JA. 1981. *A Field Guide to the Atmosphere*. Houghton Mifflin: New York, NY.

Schröder F, Kärcher B, Duroure C *et al.* 2000. On the transition of contrails into cirrus clouds. *J. Atmos. Sci.* **57**: 464–480.

Schultz DM, Kanak KM, Straka JM *et al.* 2006. The mysteries of mammatus clouds: observations and formation mechanisms. *J. Atmos. Sci.* **63**: 2409–2435.

Schultz DM, Durant AJ, Straka JM *et al.* 2008. Reply. *J. Atmos. Sci.* **63**: 1095–1097.

Schultz DM, Anderson S, Fairman JG Jr. *et al.* 2015. ManUniCast: a real-time weather and air-quality forecasting portal and app for teaching. *Weather* **70**: 180–186.

Scorer RS. 1955. Condensation trails. *Weather* **10**: 281–287.

Scorer RS. 1972. *Clouds of the World*. David and Charles: Devon, UK.

Scorer RS, Davenport LJ. 1970. Contrails and aircraft downwash. *J. Fluid Mech.* **43**: 451–464.

Sussmann R, Gierens KM. 2001. Differences in early contrail evolution of two-engine versus four-engine aircraft: lidar measurements and numerical simulations. *J. Geophys. Res.* **106**(D5): 4899–4911.

RMetS Royal Meteorological Society

Unterstrasser S. 2014. Large-eddy simulation study of contrail microphysics and geometry during the vortex phase and consequences on contrail-to-cirrus transition. *J. Geophys. Res. Atmos.* **119**: 7537–7555.

Unterstrasser S, Paoli R, Sölch I *et al*. 2014. Dimension of aircraft exhaust plumes at cruise conditions: effect of wake vortices. *Atmos. Chem. Phys.* **14**: 2713–2733.

Varney BM. 1921a. The Argonne Battle cloud. *Mon. Weather Rev.* **49**: 348–349.

Varney BM. 1921b. Cloud formation by supercharged plane. *Mon. Weather Rev.* **49**: 412.

Wegener A. 1921. Frost supersaturation (Frontstübersättigung) and cirrus. *Mon. Weather Rev.* **49**: 349.

Well ED. 1919. Clouds formed by airplanes. *Sci. Am.* **120**: 601.

Winstead NS, Verlinde J, Arthur ST *et al*. 2001. High-resolution airborne radar observations of mammatus. *Mon. Weather Rev.* **129**: 159–166.

World Meteorological Organization. 1975. *International Cloud Atlas, Volume I: Manual on the Observation of Clouds and Other Meteors*. World Meteorological Organization, No. 407. library.wmo.int/opac/index.php?lvl=notice_display&id=5357 (accessed 10 March 2016).

World Meteorological Organization. 1987. *International Cloud Atlas, Volume II*. World Meteorological Organization, No. 407. library.wmo.int/opac/index.php?lvl=notice_display&id=5358 (accessed 10 March 2016).

Correspondence to: David M. Schultz

david.schultz@manchester.ac.uk

doi:10.1002/wea.2765

Figure 1. The next generation of meteorologists. Over 75 delegates attended the Student & Early Career Conference.